9 Modeling the History Effect on Microbial Growth and Survival: Deterministic and Stochastic Approaches

József Baranyi and Carmen Pin

CONTENTS

9.1 INTRODUCTION

The objective of food safety microbiology is to eliminate or at least significantly reduce the concentration of pathogenic microbes in food and to prevent their resuscitation and multiplication. Predictive microbiology focuses on the quantitative methods used to achieve this goal.

In a mathematical sense, a predictive model is a mapping between the *environment* of the microbial cells and their *response.* While primary models describe how the microbial cell concentration changes with time in a constant environment (see Chapter 2), a secondary model (such as *D values* vs. temperature; see Chapter 3) expresses a typical parameter of the response as a function of the environmental factors. Both the environment and the response are characterized by one or more, possibly *dynamic,* variables (i.e., they may change with time during observation). Temperature changing with time is an example of a dynamic environment (see Chapter 7); growth/survival curves are examples of dynamic responses, either in constant or dynamic environments.

In accordance with the standard approach to modeling, microbial responses are studied from a distinguished time point — the *zero time* of observation. Naturally, this zero time is when the environment of the cells undergoes a sudden change. Researchers should know, or at least implicitly assume the conditions at this zero time to provide *initial values* for modeling. Such initial values are, for example, the initial composition of natural flora (in the case of food environment) or the inoculum level and initial physiological state of the studied cells. Respectively, we can speak about *actual* (current) and *previous* (historical or preinoculum) environments — the initial values are the result of the previous environment.

A major obstacle in the development of predictive microbiology is that it is difficult to acquire data at low levels of cell concentration. Currently, commonly available counting methods can only measure cell concentrations of higher than *approximately* 10 cells per gram of sample. Therefore, it is frequently problematic to validate predictive microbiology models since most of them focus on situations when the cell concentration is relatively low and the measurements are inaccurate.

Growth modeling concentrates on the early stages of microbial growth in the actual environment. As mentioned, the previous environment affects growth in the actual environment, which effect gradually diminishes after inoculation. This is called the *adjustment* process; the time during which it happens is called the *lag period.*

Death modeling deals with decay in microbial concentration having two main causes: thermal inactivation, when death is relatively fast; and nonthermal death, which is generally a much slower process. Although the physiological mechanisms of the two can be completely different, it is possible to construct mathematical models for them in an analogous way. What is more, to some extent, growth and death modeling can also be discussed analogously. Accordingly, we show some basic techniques to model the effect of history on growth and death in a parallel way.

We also present a comparative review of the applied deterministic and stochastic models. Deterministic models can always be treated as sort of "averaged out" versions of stochastic models. However, "smoothing down" the biological variability means a certain loss of information — the question is just how much. Biology itself

always has stochastic elements, but sometimes they are small enough (or we hope they are small enough) to be negligible. In this case, the applied model (and its one or more variables and processes) is reduced to be deterministic, which is simpler and easier to handle. However, such a reduction can be misleading when the random elements are significant. For example, when modeling the lag period of a population of relatively few cells (the "dormant" phase of the "log conc. vs. time curve" before exponential growth), the random effects originating from the variability among the cells cannot be ignored. Similarly, when modeling the number of survivors in an adverse environment, the stochastic variability of the resistance of individual cells can also become significant.

Many authors have studied the effect of history on the lag time before growth (Augustin et al., 2000a; Augustin and Carlier, 2000; Beumer et al., 1996; Bréand et al., 1999; Buchanan and Klavitter, 1991; Dufrenne et al., 1997; Gay et al., 1996; Hudson, 1993; Mackey and Kerridge, 1988; Membré et al., 1999; Stephens et al., 1997; Walker et al., 1990; Wang and Shelef, 1992) and on the shoulder period before exponential death (Cotterill and Glauert, 1969; Mañas et al., 2001; Ng et al., 1962; Sherman and Albus, 1923; Strange and Shon, 1964). In this chapter, we attempt to provide a simple modeling approach to take into account the history effect via the concept of initial work/damage done before the exponential growth/death phase. First, we apply a deterministic model at population level (i.e., when the population size is represented by a single continuous variable), after which we discuss similar questions at single-cell level, using stochastic processes, when the variability among individual cells is also taken into account.

9.2 MODELING THE HISTORY EFFECT AT POPULATION LEVEL (DETERMINISTIC MODELING)

9.2.1 Traditional Parameters

Throughout this chapter, $x(t)$ denotes the cell concentration at the time t, and $y(t)$ denotes its natural logarithm. The slope of the "$y(t)$ vs. time" curve is the (instantaneous) specific rate, denoted by $\mu(t)$. Its maximum value, μ_{max}, is the maximum specific rate. It is positive for growth and negative for death (Figure 9.1a and Figure 9.1b). The maximum specific rate is measured at the inflexion point of the curve, if it has a sigmoid shape (Figure 9.1a). If the model is biphasic (Figure 9.1b), then this maximum does not necessarily exist. In this case, μ_{max} is meant in an asymptotic sense: $\mu(t) \rightarrow \mu_{max}$ as $t \rightarrow \infty$. In fact, we define the biphasic class of models by the criterion that $\mu(t)$ converges monotonically from a small, $\mu(0)$ initial rate, to a finite value.

In the case of growth, the most frequently modeled parameter is the maximum specific growth rate, or one of its rescaled versions: the r_{max} maximum rate in terms of $\log_{10}$ cell concentration, or the doubling time, T_d. Note the relation between them:

$$r_{max} = \mu_{max}/\ln 10; \qquad T_d = \ln 2/\mu_{max} \tag{9.1}$$

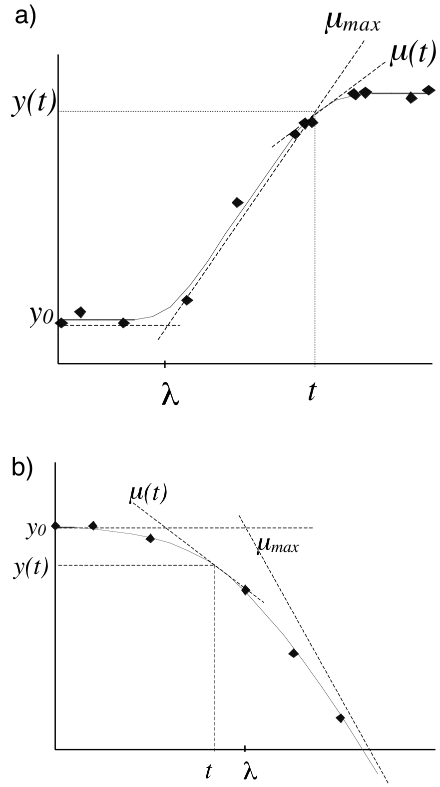


FIGURE 9.1 (a) Main parameters of a sigmoid growth curve. The maximum specific growth rate μ_{max} can be measured at the inflexion point of the curve. (b) Main parameters of a biphasic survival curve. The instantaneous specific death rate converges to a limit value $\mu_{max.}$

In the case of survival (or inactivation), instead of the analogous "halving time," it is more common to use the time to a decimal reduction, called *D* value:

$$D = -\ln 10/\mu_{max} \tag{9.2}$$

The reason for this slight inconsistency is historical: the first predictive models were created to describe thermal inactivation processes and, at high temperatures, the decimal reduction times were more practical to use than halving times.

Some authors use the maximum specific rate and some the rate of the $\log_{10} x(t)$ function, which can be obtained by an $\ln(10) \approx 2.3$ conversion factor from $\mu(t)$. Most frequently, cell concentration data are given in terms of $\log_{10}$ of the cell number per volume. However, the maximum specific rate has a more universal theoretical meaning as shown by the formulae below:

$$\frac{dy}{dt} = \frac{d(\ln x)}{dt} = \frac{dx / x}{dt}\mu(t) \tag{9.3}$$

that is,

$$\frac{\Delta x}{x} \approx \mu_{max} \Delta t \tag{9.4}$$

The left-hand side of the latter equation denotes a relative increase or decrease of the population in Δt time. Therefore, the following interpretation can be given for the maximum specific rate: the probability that, at the time t, a single cell divides (growth) or dies (death), during the small $[t, t + \Delta t]$ interval, is about $\mu(t)\Delta t$; i.e., proportional to the length of Δt, with the factor $\mu(t)$. This is a fundamental link between the specific growth rate measured at population level and the probability of division at single-cell level.

Another important, frequently modeled parameter is the lag time (for growth), or shoulder period (for survival), which is denoted by λ throughout this chapter. For sigmoid curves (Figure 9.1a), it is traditionally defined as the time when the tangent of the $y(t)$ curve with the maximum slope crosses the initial level, $y_0 = \ln x_0$ (Pirt, 1975). (It is irrelevant whether the natural logarithm or $\log_{10}$ is used to define the lag or shoulder.) For biphasic curves (Figure 9.1b), to find a good "geometrical" definition is not so straightforward as pointed out below.

The definition of lag/shoulder does not have the strong basis that would connect the parameter to a single-cell equivalent, as in the case of the specific rate. Baranyi (1998) discussed the mathematical relation between the lag of the population (as defined above) and the lag times of the participating individual cells (see later in this chapter). He showed that the population lag depends on the subsequent specific growth rate and the initial cell number, even if the individual lag times do not. Another anomaly can be shown by means of biphasic models. It is natural to expect that, if a series of tangents drawn to the $y(t)$ curves converges to a limit value (see Figure 9.1b), then the intersections with the initial y_0 level also converge, in which case the lag could be defined by the limit value. Baranyi and Pin (2001) showed a biphasic death model where this was not true; the intersection, denoting the end of the shoulder period, would not converge, as $t \to \infty$, although the specific death rate did converge.

9.2.2 Replacing the Lag Parameter with a Physiological State Parameter

For growth, the "waiting time" of the individual cells is due to an adjustment process before the exponential growth. For survival curves, the shoulder period is due to an initial resistance before exponential death (such as in the case of the multitarget theory, Hermann and Horst, 1970). As shown by Baranyi (2002), it is not easy to relate the distribution of the "waiting times" of individual cells to the apparent lag/shoulder parameter of the population, measured in the traditional way.

Baranyi and Roberts (1994) suggested that the lag should be considered as a derived parameter, a consequence of both the actual environment (via the specific growth rate), and the history of the cells (via a newly introduced parameter, the *initial physiological state* of the cells). Their method can be outlined as follows.

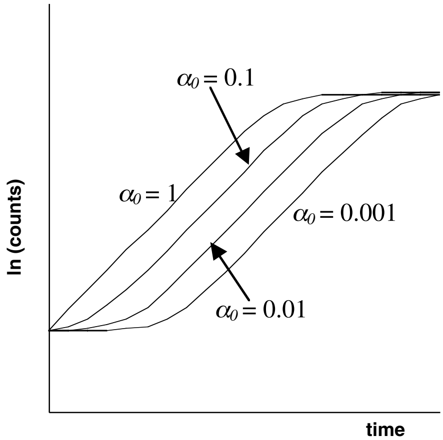


FIGURE 9.2 Interpretation of the α_0 physiological state. $h_0 = -\ln(\alpha_0) = \lambda\mu_{max}$ is the "work to be done," which is the same for different temperatures. h_0 is an initial value, as is $\ln x_0$.

Just as y_0 is an *initial* value, we can introduce another value in order to quantify the "suitability" of the population to the current environment (i.e., the history effect). Let this quantity be denoted by α_0 (which comes from the term *adjustment function,* in the original paper). Let it be a dimensionless number between 0 and 1. For growth, consider it as the fraction of the initial cells, which, without a lag, would be able to produce the same final growth as the original x_0 initial cells with a lag. (Although the real situation is not like this, it is easier to think about α_0 this way. In reality, α_0 is the mean value of the respective parameters of the individual cells. The point is, as we will see later, that it does not matter if we think of it as "α_0, the fraction of the cells that are able to grow," or "each cell is α_0-suitable.")

By simple geometry (see Figure 9.2), it can be shown that

$$\lambda = \frac{-\ln(\alpha_0)}{\mu_{max}} \tag{9.5}$$

This formula expresses our expectation that the lag time depends on both the actual environment, represented by μ_{max}, and the history of the cells, characterized by α_0. The history effect appears as an initial value, and this will be called the initial physiological state. Note that it does not represent simply the "health" of the cells, rather their suitability to the actual environment. Its extreme values are $\alpha_0 = 0$, in which case the lag is infinitely long, and $\alpha_0 = 1$, when all the cells enter the exponential phase immediately and the lag time is 0. The effect of the initial physiological state on the lag is shown in Figure 9.3.

In terms of biological interpretability, the main advantages of using α_0, instead of lag, are:

1. It is an initial value, affecting the lag, and this is in accord with our mechanistic thinking.

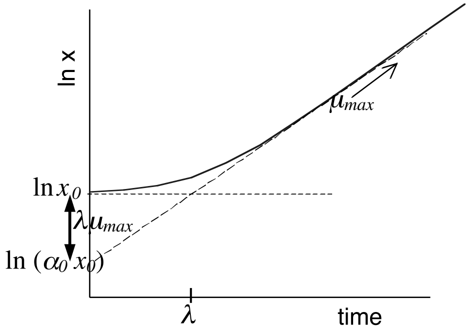


FIGURE 9.3 Depending on the α_0 physiological state, the lag can change while the maximum specific growth rate remains the same.

2. It has a very strong connection with similar parameters of the individual cells: the physiological state of the population is equal to the average of the physiological states of the initial cells, irrespective of their number (Baranyi, 1998).
3. It can be interpreted, via the individual cells, even if no traditional lag can be measured on the bacterial curve (for example, when it does not reach its inflexion point).

9.2.3 A Rescaling of the Physiological Parameter Provides a New Interpretation

An interpretation of the history effect is also possible by means of the inverse of the physiological state. Introduce $h_0 = \ln(1/\alpha_0) = -\ln \alpha_0$. It can be conceived as an initial *hurdle*, or the "work to be done" during the lag (Robinson et al., 1998; see Figure 9.2). As we see, it is the product of the lag and the maximum specific growth rate. Observe that, using the doubling time, $T_d = \ln 2/\mu_{max}$ relation, the following formula can be obtained:

$$h_0 = \ln 2 \frac{\lambda}{T_d} \tag{9.6}$$

The quantity λ/T_d is often called "relative lag" (McMeekin et al., 2002) and it is essentially the same as h_0. Some authors have reported that it is unaffected by small changes of temperature (Pin et al., 2002; Robinson et al., 1998) and pH (McKellar et al., 2002a). This can be explained as follows: the more suitable the cells are to the new environment, the less work they have to carry out to adapt. Therefore, the lag is longer at lower temperatures because the "work to be done," after the inoculation, is carried out more slowly, although the amount of work is the same (Figure 9.4). Authors studying the effect of history and actual growth conditions on the work to be done during the lag include Delignette-Muller (1998), Robinson et al. (1998), Pin et al. (2002), and Augustin et al. (2000a).

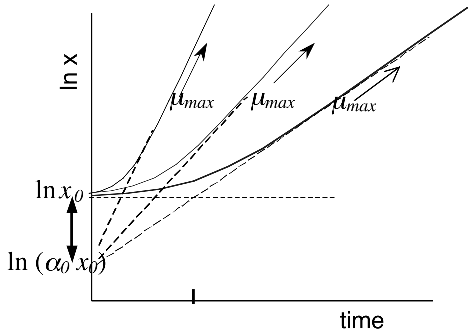


FIGURE 9.4 As the temperature decreases, the work to be done (the difference between ln x_0 and ln(α_0 x_0)) is the same, while the maximum specific growth rate μ_{max} becomes smaller and the lag becomes longer. The work to be done during the lag is also carried out at slower rates.

The parameter $h_0 = -\ln \alpha_0$, the "work to be done" before the exponential phase, plays the role of a bridge between the history and the actual environment. With an analogy, imagine that cells are crossing this bridge. If its angle is horizontal (h_0 = 0; no difficulty to overcome), then there is no lag. If it is vertical ($h_0 = \infty$), then the work to be done is infinitely big, the lag is infinitely long. On the other hand, if the temperature is higher then every movement is quicker and so is the crossing (lag), although the work to be done is the same (Figure 9.4). It can be expected that this work is smaller when adjusting to a more favorable environment than the opposite way (Delignette-Muller, 1998; Robinson et al., 1998). This theory explains why the environmental effect on the lag has always been much less accurately predicted (Dufrenne et al., 1997; McKellar et al., 2002b; McMeekin et al., 2002; Robinson et al., 1998; Whiting and Bagi, 2002) than the specific growth rate. The lag also depends on the history, the details of which often have not even been recorded, let alone taken into account in the model.

9.3 MODELING THE HISTORY EFFECT AT SINGLE-CELL LEVEL (STOCHASTIC MODELING)

9.3.1 Nature of Stochastic Modeling

Finer details of the effect of history on growth/death can be seen through a closer look at the distribution of the division/survival times of individual cells. As mentioned in Section 9.1, if only deterministic models are used to describe responses of microbial populations then the variability among single cells is ignored. This is a problem because predicting microbial variability is increasingly important for Quantitative Microbial Risk Assessment. This variability of the responses increases under stress conditions, which makes predictions even less accurate.

A characteristic feature of stochastic modeling is that it sometimes provides unexpected results. An example of this is the relation between the doubling time of a growing population and the average generation time of the individual cells in the

population. Depending on the distribution of the individual generation times, these two quantities can be markedly different. If the generation times follow the classical exponential distribution, then their average is $1/\mu_{max}$, while the doubling time is known to be $\ln 2/\mu_{max}$, where μ_{max} is the (constant) maximum specific growth rate of the population. Baranyi and Pin (2001) described the exponential growth as a Poisson birth process and showed that with this approach the doubling time depends on the number of cells, from $1/\mu_{max}$, when the number of cells is 1, converging to $\ln 2/\mu_{max}$, when the number of cells increases.

9.3.2 Physiological State and Lag Parameters for Single Cells

Let $N(t)$ be the *number* of cells in a defined space, at the time t (remember, that $x(t)$ denoted the *concentration* of the cells). Let the lag for the ith cell of the initial population be denoted by τ_i ($i = 1,2,\ldots, N$). We assume that they are identically distributed independent random variables, and their mean value is τ. Note that τ_i is less than the time to the first division of the ith cell, which also includes the first generation time.

Define the physiological states α_i ($i = 1,2,\ldots,N$) for the individual cells by $\alpha_i = \exp(-\mu_{max}\tau_i)$, analogously to the deterministic theory. A basic theorem of Baranyi (1998) is that the average of the individual physiological states is the same as the physiological state of the population, irrespective of the distribution of the individual lag times. Moreover, if $\lambda(N)$ denotes the (traditionally defined) lag of the population consisting of N cells, then

$$\lambda(N) = -\frac{1}{\mu}\ln\frac{\sum_{i=1}^{N}\alpha_i}{N} = -\frac{1}{\mu}\ln\frac{\sum_{i=1}^{N}e^{-\mu\tau_i}}{N} \tag{9.7}$$

This formula is demonstrated in Figure 9.5. The more cells there are in the inoculum, the shorter is the expected population lag, converging to a limit value, λ_{min}. Notice that the correct model for single-cell-generated curve is bi-phasic; the curvature for higher inoculum is caused by the distribution of the individual lag times.

Various authors have reported that at a very low inoculum (approximate to 1 cell per total volume of sample), the lag time is longer than expected (Augustin et al., 2000b; Gay et al., 1996; Stephens et al., 1997). However, as the above formula shows, this finding can also be explained by statistical means without extra biological assumptions. The lag time decreases with the initial cell number because the exponentially growing subgenerations of the cells with the shortest lag times will quickly dominate the whole population.

In particular, Baranyi and Pin (2001) showed the mathematical relation between the respective parameters (mean and variance) of the individual lag times and those of the population consisting of N cells. From these formulae, the distribution of individual lag times is *per se* different from the distribution of the population lag times. This was confirmed by the observation of Stephens et al. (1997) on heat-

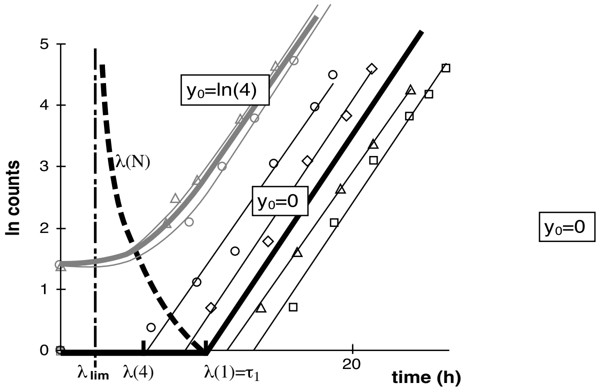


FIGURE 9.5 Simulating four single-cell-generated growth curves ($y_0 = 0$) growing separately, and two separate growth curves generated by four cells each ($y_0 = \ln 4$). The traditional lag times λ of the subpopulations are estimated by curve fitting. Observe that the $\lambda(N)$ mean population lag converges to a limit value λ_{lim} while its variance (the spread of the growth curves as a function of their inoculum) converges to zero (see Figure 9.6). Symbols: simulated points; continuous thin lines: fitted curves; continuous thick lines: expected curves.

injured *Salmonella* cells. The calculations provided another reason why the lag time should not be considered as a primary growth parameter but as the result of the initial physiological state (α_0), the inoculum size and the maximum specific growth rate.

Smelt et al. (2002) estimated the population lag as the minimum of the individual lag times. Our formula shows that the population lag is greater than the minimum of the individual lag times, but closer to it than to the arithmetical mean.

9.3.3 A Simulation Program

To demonstrate the effect of the inoculum on the distribution of the population lag, we developed a simulation program. One hundred growth curves from different inoculum sizes were generated. The distribution functions used by the simulation were based on the theory of Baranyi and Pin (2001).

We assumed that the individual lag times followed the gamma distribution, with the parameters p and v, so the mean individual lag is $\tau = p/v$. The biological interpretation of this scenario is that the cells have to carry out p consecutive tasks, and the times required by the individual tasks are independent, exponentially distributed random variables, with the parameter v (i.e., the average time required for each task was $1/v$).

The parameter p represented the amount of work to be done during the lag time ($h_0 = p$). Partly for simplicity, partly for mechanistic reasons, $v = \mu_{max}$ was assumed. The generation times, g_i, of individual cells, after the lag phase, followed the exponential distribution with the parameter μ_{max}.

With the usual terminology for stochastic processes, the initial state of the system is $(N,0)$, meaning that there are N cells in the lag phase and 0 in the exponential phase at the starting time (t_0). The time t_1 of the first division in the population is

that of the cell with the smallest value for the sum of its lag time, τ_i, and its first generation time, g_i.

$$t_1 = \min(\tau_1 + g_1, \dots \tau_N + g_N)$$

After the first division, $N - 1$ cells remain in lag phase while 2 cells are in exponential growth phase. Thus the state of the system is $(N - 1, 2)$. The time t_2 of the second division will be the minimum of the first division times among the $N - 1$ cells remaining in the lag phase and the division times of the two daughter cells:

$$t_2 = \min(\tau_1 + g_1, \dots \tau_{N-1} + g_{N-1}, t_1 + g_{N+1}, t_1 + g_{N+2})$$

This second division can happen to a cell in exponential or in lag phase.

1. If a cell in lag phase divides, then the state of the system will be $(N - 2, 4)$ and the time of the third division will be $t_3 = \min(\tau_1 + g_1, \dots, \tau_{N-2} + g_{N-2}, t_1 + g_{N+1}, t_1 + g_{N+2}, t_2 + g_{N+3}, t_2 + g_{N+4})$.
2. If a cell in exponential phase divides, then the system jumps into the state $(N - 1,3)$. Apart from numbering the daughter cells, the time to the third division will be $t_3 = \min(\tau_1 + g_1, \dots, \tau_{N-1} + g_{N-1}, t_1 + g_{N+2}, t_2 + g_{N+3}, t_2 + g_{N+4})$.

The iteration can be continued in a similar manner and this is what our simulation program did, until the population had a given number of cells. One hundred growth curves were generated for each selected inoculum size. The parameters h_0 and μ_{max} were chosen close to practical values: $h_0 = 4$ and $\mu_{max} = 0.5$ h^{-1}. Thus the gamma parameters to simulate the individual lag times were $p = 4$ and $v = 0.5$ h^{-1} (mean individual lag = 8 h) and the parameter of the exponential distribution to simulate the individual generation times was 0.5 h^{-1} (mean generation time = 2 h). The traditionally interpreted lag time of each population curve was estimated by fitting a biphasic (no upper asymptote) version of the model of Baranyi and Roberts (1994). Figure 9.5 shows typical examples of the generated population curves (originating from one and four cells). As can be seen, in the case of a single initial cell, when the inoculum is $\ln x = 0$, the population lag (λ, measured by the tangent to the exponential phase) is close to the theoretical individual lag ($\tau_I = 8$ h).

If the inoculum size increases then, from the formula

$$\lambda(N) \xrightarrow{N \to \infty} \lambda_{\lim} = \frac{p}{\mu} Ln\left(1 + \frac{\mu\tau}{p}\right) \tag{9.8}$$

the population lag converges to $\lambda_{\lim} = 8 \cdot \ln 2 = 5.54$. This convergence is shown in Figure 9.5. Figure 9.6 shows the distribution of the population lag times as a function of the inoculum size.

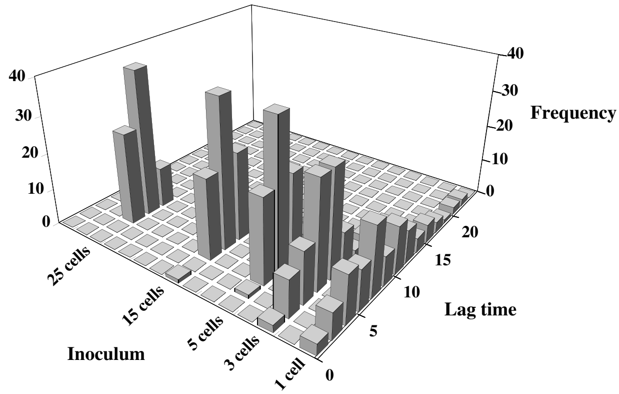


FIGURE 9.6 As the inoculum size increases, the population lag time decreases, converging to a limit value. Its variance converges to zero.

9.3.4 Lag/Survival Distribution of Single Cells and Lag/Shoulder of Population Curves

A general result from Baranyi (2002) connects the expected population growth curve with the distribution of single-cell kinetics:

$$x(t) = N\left(\int_0^t e^{\mu\cdot(t-s)} f(s)ds + \int_t^\infty f(s)ds\right) \tag{9.9}$$

where $f(t)$ denotes the (common) probability density function (pdf) of the individual lag times. It is analogous to the formula of Körmendy et al. (1998) for death curves:

$$x(t) = N\int_0^\infty e^{-s\cdot t} g(s)ds \tag{9.10}$$

where $g(s)$ is the probability density function of the individual cells' death rate (i.e., the reciprocal of their survival time). The big difference is that while the probability distribution of the individual survival times determines the whole death curve (actually by a Laplace transformation, as the formula shows) that of the individual lag times does not. In both models, the first compartments are "dormant" states, but the second ones are totally different: for growth, it is the state of exponential growth, characterized by the specific growth rate; for survival curves, it is a "death phase" without any parameter.

The formulae above represent a one-to-one mapping between the $f(t)$ distribution and the population growth/death curve. The problem is that, in practice, this mapping works only in one direction. The expected population curve can be easily derived from the distribution of the individual lag times, but vice versa it would need

unrealistically accurate data. This is an example where the performance of stochastic techniques is much better than that of their deterministic counterparts.

9.3.5 History Effect on the Shoulder Periods of Survival Curves

For survival curves, with the notations as above, let τ_i be the time for the *i*th cell to die, and assume that it is distributed exponentially, with the mean value τ (pure Poissonian death process). In this case, $F(t) = 1 - e^{-t/\tau}$, so the survival curve is $y(t) = \ln N - t/\tau$. Therefore, in this case, the survival curve is linear and there is no shoulder parameter: $\lambda = 0$.

Analogously with our approach to modeling the distribution of individual lag times for growth, consider now the situation when τ_i ($i = 1,\ldots, N$) follow the gamma distribution, with the parameters $p \geq 1$ and $\nu > 0$, where the expected value of the survival time for a cell is $\tau = p/\nu$. This is interpreted by Baranyi and Pin (2001) in the following way: the cell needs *p* damaging hits (see the multihit theory in Casolari, 1988), and the times θ_j ($j = 1,\ldots, p$) between the hits are independent, exponentially distributed variables, with a common mean value $\theta = 1/\nu$. Then the survival time of the *i*th cell is

$$\tau_i = \sum_{j=1}^{p} \theta_j \tag{9.11}$$

therefore τ_i ($i = 1,\ldots, N$) are gamma distributed. In this case, as shown by the authors, the derivative of $y(t)$ converges to a constant, namely ν, the limit shoulder still does not exist if $p > 1$. In practice, the shoulder would be measured by ν and the smallest detectable value of $y(t)$, which means that the shoulder measurement would depend on the precision of the measurement method! This inconsistency makes the shoulder parameter unsuitable for modeling. Instead, the *p* parameter quantifying the "damage to be done" should be modeled, which is analogous to the h_0 parameter for growth curves.

Another well-known interpretation of the shoulder is the so-called multitarget model (Hermann and Horst, 1970). According to that, a cell has *p* targets that are being hit synchronously (not consecutively as in the previous case). The times needed to destroy the targets, θ_j ($j = 1,\ldots, p$), are independent, exponentially distributed variables with the common mean value of $1/\nu$ and the cell is live until all targets are inactivated. Therefore, the survival time of the *i*th cell is

$$\tau_i = \max_{1 \leq j \leq p} \theta_j \tag{9.12}$$

and $F(t) = (1 - e^{-\nu t})^p$, where $p \geq 1$. The population survival curve is now

$$y(t) = \ln N + \ln(1 - (1 - e^{-\nu t})^p) \tag{9.13}$$

which converges to the

$$y_a(t) = \ln N - \nu \cdot (t - \ln p/\nu) \tag{9.14}$$

linear asymptote. Therefore, the limit shoulder parameter can be calculated as

$$\lambda = \ln p/\nu \tag{9.15}$$

This shows another analogy to the modeling of the history effect on growth: the "ln *p*" quantity could be used to characterize the initial "damage to be done," and the shoulder period depends on the magnitude of the initial damage and on the rate as the damage is being done.

9.4 CONCLUDING REMARKS

In this chapter, we showed that the history effect can be quantified either by the "initial physiological state" or the "work to be done" parameters; they are simply rescaled versions of each other. The traditional lag parameter has become a derived one, useful for static conditions only. By introducing a variable for the rate at which the work is carried out before the exponential phase, the model can be used for dynamic conditions, too. This concept was successfully applied in a series of papers (Baranyi et al., 1995, 1996) describing the entire bacterial growth profile (not only the exponential phase) under fluctuating conditions.

The priority of α_0 is purely a modeling concept; it does not mean that when fitting a bacterial growth curve, α_0 and not the lag should be estimated. The formula $\lambda = -\ln\alpha_0/\mu_{max}$ to calculate the lag expresses the view that both the history and the current environment influence the lag. This has practical consequences when developing more complex, dynamic models or, for example, when developing predictive software packages. These commonly require the user to provide values for the environmental factors, from which the maximum specific rate (or one of its rescaled versions) and a *default* lag are predicted. If the user gives the inoculum, then the whole growth curve can be constructed, too. What our theory suggests is that it is not only the inoculum that cannot be predicted from the current environment, but also the initial physiological state, α_0. This is shown in Figure 9.2: there are two independent initial points on the *y* axis:

1. An inoculum value (y_0)
2. A point through which the tangent drawn to the inflexion will pass (which is $h_0 = -\ln\alpha_0$ lower than the inoculum)

Sometimes the value of the initial physiological state should be simply $\alpha_0 = 1$, expressing the fact that the preinoculation conditions are the same as the current environment.

As has been mentioned, many features of the shoulder period before the exponential death phase can be discussed analogously to those of the lag period before

the exponential growth phase. Baranyi and Pin (2001) showed that the multitarget theory of inactivation (Hermann and Horst, 1970), modeling the shoulder before the exponential death rate, provides a parallel between the initial "damage to be done" for death and the h_0 "work to be done" for growth. The "bridge" between the history and the current environment is characterized by h_0 either for growth (Figure 9.2) or death (the mirror image of Figure 9.2).

The question can be raised of why the distribution of individual lag times is important once different distributions can result in practically the same population curve. The answer lies in the interest of Quantitative Microbial Risk Assessment in the distribution of the quantity "time to a certain level" (such as time to infective dose or time to legally allowed concentration). The distribution of that time depends heavily on the distribution of individual lag times.

Modeling the effect of history is more efficient with stochastic techniques, but also more data- and maths-demanding. Deterministic models are able to produce "averaged out" solutions only, and studying the variability around those predictions is vital in Quantitative Microbial Risk Assessment.

ACKNOWLEDGMENT

The authors are indebted to Susie George for preparing the manuscript. This work was funded by the EC project QLRTD-2000-01145 and the IFR project CSG 434.1213A.

REFERENCES

Augustin, J.C., L. Rosso, and V. Carlier. 2000a. A model describing the effect of temperature history on lag time for *Listeria monocytogenes. Int. J. Food Microbiol*. 57, 169–181.

Augustin, J.C., A. Brouillaud Delattre, L. Rosso, and V. Carlier. 2000b. Significance of inoculum size in the lag time of *Listeria monocytogenes. Appl. Environ. Microbiol*. 66, 1706–1710.

Augustin, J.C. and V. Carlier. 2000. Mathematical modelling of the growth rate and lag time for *Listeria monocytogenes. Int. J. Food Microbiol.* 56, 29–51.

Baranyi, J. 1998. Comparison of stochastic and deterministic concepts of bacterial lag. *J. Theor. Biol.* 192, 403–408.

Baranyi, J. 2002. Stochastic modelling of bacterial lag phase. *Int. J. Food Microbiol*. 73, 203–206.

Baranyi, J. and C. Pin. 2001. A parallel study on bacterial growth and inactivation. *J. Theor. Biol*. 210, 327–336.

Baranyi, J. and T.A. Roberts. 1994. A dynamic approach to predicting bacterial growth in food. *Int. J. Food Microbiol*. 23, 277–294.

Baranyi, J., A. Jones, C. Walker, A. Kaloti, and B.M. Mackey. 1996. A combined model for growth and thermal inactivation of *Brochothrix thermosphacta. Appl. Env. Microbiol*. 62, 1029–1035.

Baranyi, J., T.P. Robinson, A. Kaloti, and B.M. Mackey. 1995. Predicting growth of *Brochothrix thermosphacta* at changing temperature. *Int. J. Food Microbiol*. 27, 61–75.

Beumer, R.R., M.C. te Giffel, E. de Boer, and F.M. Rombouts. 1996. Growth of *Listeria monocytogenes* on sliced cooked meat products. *Food Microbiol*. 13, 333–340.

Bréand, S., G. Fardel, J.P. Flandrois, L. Rosso, and R. Tomassone. 1999. A model describing the relationship between regrowth lag time and mild temperature increase for *Listeria monocytogenes. Int. J. Food Microbiol*. 46, 251–261.

Buchanan, R.L. and L.A. Klavitter. 1991. Effect of temperature history on the growth of *Listeria monocytogenes* at refrigeration temperatures. *Int. J. Food Microbiol*. 12, 235–246.

Casolari, A. (1988). Microbial death. In *Physiological Models in Microbiology. Vol. II,* Bazin, M.J. and Prosser, J.I., Eds. CRC Press, Boca Raton, FL, Ch. 7.

Cotterill, O.J. and J. Glauert. 1969. Thermal resistance of *Salmonellae* in egg yolk products containing sugar or salt. *Poult. Sci*. 48, 1156–1166.

Delignette-Muller, M.L. 1998. Relation between the generation time and the lag time of bacterial growth kinetics. *Int. J. Food Microbiol*. 43, 97–104.

Dufrenne, J., E. Delfgou, W. Ritmeester, and S. Notermans. 1997. The effect of previous growth conditions on the lag phase time of some foodborne pathogenic microorganisms. *Int. J. Food Microbiol*. 34, 89–94.

Gay, M., O. Cerf, and K.R. Davey. 1996. Significance of pre-incubation temperature and inoculum concentration on subsequent growth of *Listeria monocytogenes* at 14°C. *J. Appl. Bacteriol*. 81, 433–438.

Hermann, D. and J. Horst. 1970. *Molecular Radiation Biology.* Springer, Berlin.

Hudson, J.A. 1993. Effect of pre-incubation temperature on the lag time of *Aeromonas hydrophila. Lett. Appl. Microbiol*. 16, 274–276.

Körmendy, I., L. Körmendy, and A. Ferenczy. 1998. Thermal inactivation kinetics of mixed microbial populations. A hypothesis paper. *J. Food Eng.* 38, 439–453.

Mackey, B.M. and A.L. Kerridge. 1988. The effect of incubation temperature and inoculum size on growth of *Salmonellae* in minced beef. *Int. J. Food Microbiol*. 6, 57–65.

Mañas, P., R. Pagan, I. Leguerinel, S. Condon, P. Mafart, and F. Sala. 2001. Effect of sodium chloride concentration on the heat resistance and recovery of *Salmonella typhimurium. Int. J. Food Microbiol*. 63, 209–216.

McKellar, R.C., X. Lu, and K.P. Knight. 2002a. Growth pH does not affect the initial physiological state parameter (p_0) of *Listeria monocytogenes* cells. *Int. J. Food Microbiol*. 73, 137–144.

McKellar, R.C., X. Lu, and K.P. Knight. 2002b. Proposal of a novel parameter to describe the influence of pH on the lag phase of *Listeria monocytogenes. Int. J. Food Microbiol.* 73, 127–135.

McMeekin, T.A., J. Olley, D.A Ratkowsky, and T. Ross. 2002. Predictive microbiology: towards the interface and beyond. *Int. J. Food Microbiol*. 73, 395–407.

Membre, J.M., T. Ross, and T. McMeekin. 1999. Behaviour of *Listeria monocytogenes* under combined chilling processes. *Lett. Appl. Microbiol*. 28, 216–220.

Ng, H., J.L. Ingraham, and A.G. Marr. 1962. Damage and depression in *Escherichia coli* resulting from growth at low temperatures. *J. Bacteriol*. 84, 331–339.

Pin, C., G.D. García de Fernando, J.A. Ordóñez, and J. Baranyi. 2002. Analysing the lag-growth rate relationship of *Yersinia enterocolitica. Int. J. Food Microbiol*. 73, 197–201.

Pirt, S.J. 1975. *Principles of Microbe and Cell Cultivation*. Blackwell, London.

Robinson, T.P., M.J. Ocio, A. Kaloti, and B.M. Mackey. 1998. The effect of the growth environment on the lag phase of *Listeria monocytogenes. Int. J. Food Microbiol*. 44, 83–92.

Sherman, J.M. and W.R. Albus. 1923. Physiological youth in bacteria. *J. Bacteriol*. 8, 27–139.

Smelt, J.P.P.M., G.D. Otten, and A.P. Bos. 2002. Modelling the effect of sublethal injury on the distribution of the lag times of individual cells of *Lactobacillus plantarum. Int. J. Food Microbiol*. 73, 207–212.

Stephens, P.J., J.A. Joynson, K.W. Davies, R. Holbrook, H.M. Lappinscott, and T.J. Humphrey. 1997. The use of an automated growth analyser to measure recovery times of single heat-injured *Salmonella* cells. *J. Appl. Microbiol*. 83, 445–455.

Strange, R.E. and M. Shon. 1964. Effects of thermal stress on viability and ribonucleic acid of *Aerobacter aerogenes* in aqueous suspension. *J. Gen. Microbiol*. 34, 99–114.

Walker, S.J., P. Archer, and J.G. Banks. 1990. Growth of *Listeria monocytogenes* at refrigeration temperatures. *J. Appl. Bacteriol*. 687, 157–162.

Wang, C. and L.A. Shelef. 1992. Behaviour of *Listeria monocytogenes* and the spoilage microflora in fresh cod fish treated with lysozyme and EDTA. *Food Microbiol*. 9, 207–213.

Whiting, R.C. and L.K. Bagi. 2002. Modelling the lag phase of *Listeria monocytogenes. Int. J. Food Microbiol*. 73, 291–295.